Estimating the Aggregate Interference from High-Density Fixed Service Emitters to Deep-Space Earth Stations

Ted Peng,* Peter Kinman,† Selahattin Kayalar,* and Christian Ho*

This article introduces a method to estimate the aggregate interference from future high-density fixed service emitters to deep-space Earth stations. In this method, the area surrounding the deep-space Earth station is geometrically partitioned, and this partition is used to model the correlation of interferences. The propagation losses are calculated considering the terrain and the atmospheric conditions. The method uses statistical models and their numerical approximations to estimate the aggregate interference. This method is applied to the areas surrounding the deep-space Earth stations of NASA's Deep Space Network (DSN) at Goldstone–USA, Robledo–Spain, and Tidbinbilla–Australia to estimate the aggregate interference received from any given geographical distribution of high-density fixed service emitters in the 37-GHz band. It also provides a basis to establish emission limits for these emitters to ensure compatibility of operation between the high-density fixed service and the space research service.

I. Introduction

In the Radio Regulations of the International Telecommunication Union–Radiocommunication Sector (ITU-R), the 31.8- to 32.3-GHz and 37- to 38-GHz bands are allocated to space research service (SRS), space-to-Earth, on a primary basis. The same bands are also allocated to the fixed service on a primary basis and are available for high-density applications in the fixed service (HDFS).

The SRS, deep space, is supported worldwide by a few Earth stations that are highly sensitive to interference and are protected by stringent protection criteria [1,2]. Resolution 75 (WRC 2000) of the Radio Regulations has recognized that emissions from HDFS emitters distributed in areas surrounding a deep-space Earth station can potentially interfere with it. This aggregate interference from the HDFS emitters to the deep-space Earth station needs to be quantified.

* Communication Architectures and Research Section.
† California State University at Fresno.

The research described in this publication was carried out by the Jet Propulsion Laboratory, California Institute of Technology, under a contract with the National Aeronautics and Space Administration.

The calculation of aggregate interference in general is a difficult problem. The ITU-R provides statistical characterizations of the propagation loss between a single transmitter and a receiver for several different propagation mechanisms. However, calculation of aggregate interference from multiple transmitters requires characterization of the statistical dependence between propagation losses associated with these transmitters. Such characterization is not available from the ITU-R or elsewhere in the engineering literature. Therefore, heuristic models must be used, and consequently the results will be approximate.

Aggregate equivalent isotropically radiated power (AEIRP) for a group of transmitters has been defined by the ITU-R [3]. AEIRP is the algebraic sum of the equivalent isotropically radiated powers (EIRP) of individual transmitters in the direction of propagation toward the victim antenna. This definition is practical when the propagation loss between a transmitter and a receiver is approximately the same for all transmitters in the group. This will often be the case when the group of transmitters occupies an area with dimensions much smaller than the distance to the receiver. In such a case, the received power spectral density (PSD) can be calculated approximately as from a single transmitter with an EIRP equal to the AEIRP so calculated.

In order to estimate the aggregate interference from all HDFS emitters surrounding a deep-space Earth station, it is necessary to characterize first the propagation loss from an emitter to the deep-space Earth station. The propagation loss depends on terrain and on atmospheric conditions. The dependence on terrain can be modeled accurately by using high resolution terrain heights. The dependence on atmospheric conditions can be modeled statistically using experimentally determined equations [4,5].

One example of calculating the aggregate interference is presented in [6] for the radio astronomy Earth stations. In the case of radio astronomy, the random propagation losses associated with all the emitters are assumed to be statistically correlated, regardless of their locations. This assumption is reasonable for radio astronomy service since the protection criterion for radio astronomy requires that the aggregate interference not exceed a threshold PSD level for more than 2 percent of the time [6], which is rather high. On the other hand, the protection criteria of the SRS, deep space, as given in Section II, specify a very low exceedence percentage of 0.001 percent, which is about 5 min total in 1 yr. It is unrealistic to suppose that propagation paths of all emitters surrounding the deep-space Earth station will experience their lowest loss at the same time. For this reason, the model used for estimating the aggregate interference to a radio astronomy Earth station is not appropriate for a deep-space Earth station.

In this article, a method is proposed for the estimation of aggregate interference from the HDFS emitters to a deep-space Earth station. The method is applied to the Deep Space Network (DSN) sites at Goldstone–USA (California), Robledo–Spain (near Madrid), and Tidbinbilla–Australia (near Canberra) for the 37-GHz band to illustrate the procedures and potential implications.

II. SRS Deep Space Protection

During launch, cruise, and science phases, a deep-space mission faces many important events, such as encounters, flybys, probe separation, orbit insertion, or entry, descent, and landing. These so-called critical events can last from a few minutes to a few hours. During a critical event, especially a short one, interference lasting a few seconds could jeopardize the mission. Therefore, deep-space missions have very stringent protection criteria.

ITU-R Recommendations given in [1,2] provide protection criteria for the deep-space research for the bands 32 GHz and 37 to 38 GHz. In these recommendations, the importance of critical events in deep-space research and the extreme sensitivity of the deep-space Earth station are recognized. No man-made interference is allowed in the line of sight, and interferences received from the sources over the horizon are not to exceed the specified PSD protection levels for more than 0.001 percent of the time. These PSD protection levels for SRS are specified to be –216 dBW/Hz for the 31.8- to 32.3-GHz band and –217 dBW/Hz for the 37- to 38-GHz band.

III. Propagation Losses

Propagation loss is calculated using the mathematical models provided in [4]. These models depend on atmospheric and geographical parameters along the path of interference. Since the deep-space Earth stations are more or less surrounded by hills, the interfering signals from the terrestrial sources on the other side of the hills must propagate over the hills. The interfering signal from a terrestrial emitter may propagate to the respective deep-space Earth station through diffraction, tropospheric scattering, and ducting/layer reflection mechanisms [7]. Among the three mechanisms, ducting/layer reflection presents the highest propagation loss in almost all areas around the three DSN sites. Therefore, in the following analysis, the losses due to the ducting/layer reflection mechanism are ignored. Accurate propagation loss evaluations can only be obtained by calculating these losses from actual terrain data. In [7], the propagation losses for the surrounding areas within 300 km of DSN sites at Goldstone–USA, Robledo–Spain, and Tidbinbilla–Australia are calculated using terrain data with a resolution of 1 deg in azimuth angle, 100 m in the radial direction, and 1 m in vertical height. This study presumes a 70-m receive antenna, because these antennas are the tallest of the DSN and, hence, will be most susceptible to interference arriving from transhorizon emitters. The height of the electrical center of the receive antenna is 37 m, and that of the transmit antenna is assumed to be 15 m. The same propagation losses given in [7] are used in this study.

IV. Aggregate Interference Calculation

To introduce the interference problem, we depict in Figure 1 a deep-space Earth station surrounded by many HDFS emitters. In Figure 1 we also show a mountain that separates most of the HDFS emitters from the deep-space Earth station. These emitters use directional antennas pointing toward other emitters in the same service area. The problem is how to estimate the interference received by the deep-space Earth station from these emitters.

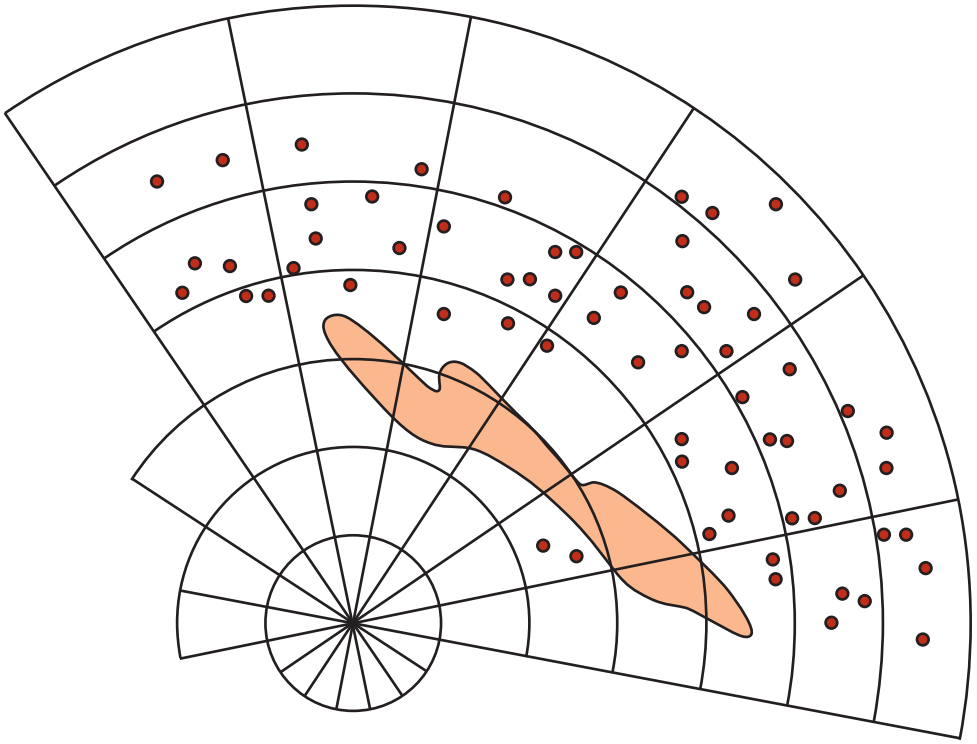

Figure 1. Distribution of HDFS emitters around a deep-space Earth station.

In general, for a given pointing direction of the receive antenna, the interference power spectral density received by the deep-space Earth station can be expressed as

$$S = \sum_{i=1}^{N_e} E_i \cdot \frac{1}{L_i(p_i)} \cdot G_i \tag{1}$$

where S is the received interference power spectral density (W/Hz), N_e is the number of HDFS emitters, E_i is the EIRP spectral density of emitter[i] toward the deep-space Earth station (W/Hz), G_i is the receiver antenna gain toward emitter[i] with a gain pattern as given in [8], and $L_i(p_i)$ is the p_i-th percentile of the propagation loss for emitter[i] due to intervening terrain and atmospheric conditions, defined to mean $Prob.\{Loss \leq L_i(p_i) = p_i\,\%$. As the antenna pointing direction changes, this equation needs to be reevaluated.

Note that Equation (1), although simple, is very difficult to apply for calculating the HDFS interference, since the number of emitters is very large, emitter EIRP spectral densities toward the deep-space Earth station are in some cases not known, and the propagation losses depend on the intervening terrain and the atmospheric conditions. Note that each emitter has been assigned a different statistical percentile (p_i) to represent the variability of the atmospheric conditions for each emitter. Since the propagation losses are varying randomly, the received interference PSD is a random variable, and can best be described by a probability distribution. If the propagation losses for the emitters are assumed to be statistically independent and known, then the probability distribution of received interference power spectral density can theoretically be obtained by convolving the underlying distributions. It can also be generated numerically by Monte Carlo simulations. Both of these methods,

however, are very intensive and time consuming. In general, the propagation losses are partially correlated and the underlying probability distributions are too complex to be tractable.

The interference PSD [Equation (1)] is random and requires a statistical characterization. However, as mentioned above, an exact statistical characterization is difficult, if not impossible, because of the large number of emitters and the complicated nature of the random propagation losses. Therefore, an approximate model is required in practice, which will sort the emitters according to the following guidelines. Emitters in close proximity (i.e., within a few kilometers) to each other will be regarded as having the same propagation loss to the deep-space Earth station, and emitters located at approximately the same azimuth as viewed from the deep-space Earth station will be regarded as experiencing a common receive antenna gain. Then, emitters will be assigned to groups (called *zone groups* in the next section), within which the propagation losses are modeled as perfectly correlated. Thus, the approximate model to be employed involves a geometric partition of the area surrounding the deep-space Earth station.

V. Geometric Partition of the Surrounding Area

To introduce a simple model for the interference from HDFS emitters to a deep-space Earth station, we begin by partitioning the area surrounding the deep-space Earth station. As such, we expect to reduce the complexity of computation by grouping emitters together that experience a common gain from the deep-space Earth station antenna and a high correlation of propagation losses. To this end, the surrounding area is first partitioned into sectors, using the deep-space Earth station as the apex of every sector, and then each sector is partitioned into zones as shown in Figure 2.

In Figure 2, the emitters in the same zone are replaced with a single equivalent emitter located at the geometric center of the zone. Note that this model allows us to include all the populated zones in any sector around the deep-space Earth station in the interference analysis.

A. Sectors

The area surrounding the deep-space Earth station is first partitioned into sectors, using the deep-space Earth station as the apex of every sector. The radial length of the sector is taken to be 300 km. The azimuth angle span of the sector is chosen to be sufficiently small such that all of the interference arriving at the receiver from any transmitter in a given sector experiences approximately the same receive antenna gain. The interference from two different sectors, even adjacent sectors, will, in general, experience different receive antenna gains. Most importantly, the propagation losses to the deep-space Earth station from emitters in different sectors are considered statistically independent. All sectors are assumed to have the same azimuthal width. In this article, the sector width is taken to be 1 deg. Every integer value of azimuth (in degrees, as measured from the deep-space Earth station) is taken as the centerline for a sector. Thus, the area surrounding the deep-space Earth station

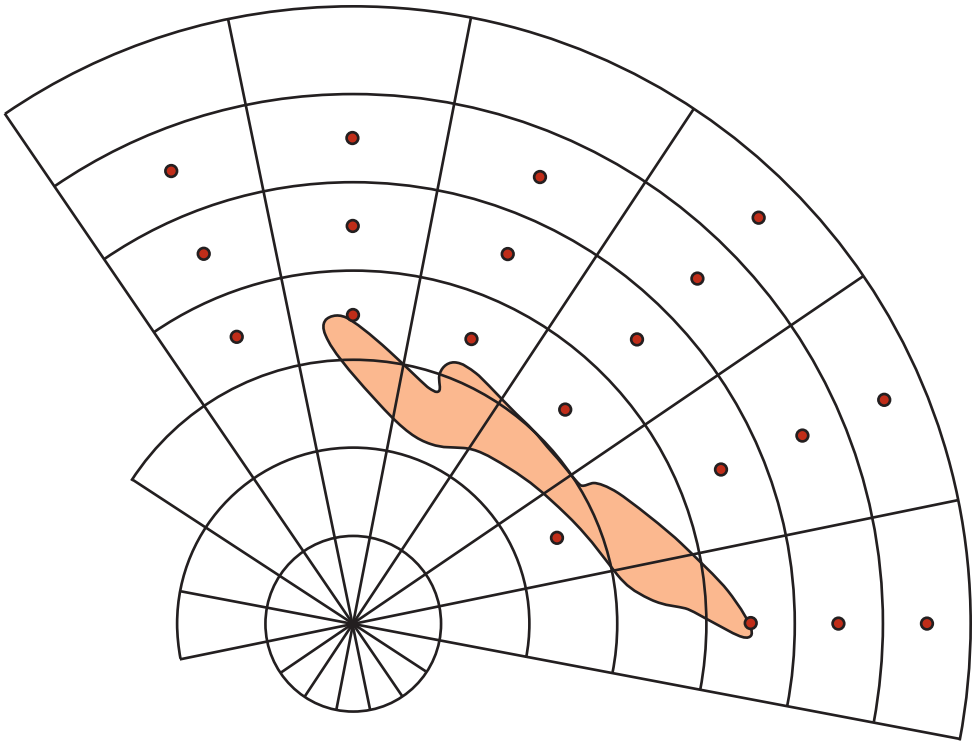

Figure 2. Sectors, zones, and zone groups. Emitters in the same zone are replaced with a single equivalent emitter at the center of the zone.

is partitioned into 360 sectors. In this article, the integer value of the azimuth of the sector centerline is used as an identifier for the sector.

B. Zones

Each sector is partitioned into zones. Each zone is chosen to be sufficiently small that the propagation loss to the deep-space Earth station is approximately the same for all emitters located within the zone. An AEIRP spectral density can then be calculated as the algebraic sum of the EIRP spectral densities of the emitters within the zone in the direction of propagation toward the deep-space Earth station. If the radiation parameters of the emitters are known, including transmitted power and antenna locations and directions, then the AEIRP can be calculated precisely. If the parameters are not given, especially the antenna orientations, estimation methods have been suggested [3], where the fixed service terminals in the zone are point-to-point and the antenna boresight angles of the emitters are random. In this study, the zones are defined to have radial length of 4 km. Since we have taken the sectors to have a radial length of 300 km, there are 75 zones in one sector.

C. Zone Groups

In general, the zones in a sector are defined to belong to the same zone group. However, if a mountain is present within a sector, then it will be necessary to divide the zones in that

sector into two zone groups, because zones on one side of the mountain experience a very different propagation loss than the zones on the other side in the direction of the deep-space Earth station.

It is assumed that the propagation losses associated with all zones in a zone group are perfectly correlated. This modeling assumption is justified on the basis that the propagation paths from all emitters in a zone group experience a similar terrain profile. In the case of troposcattering, the energy directed toward the deep-space Earth station from all emitters in a zone group are scattered in essentially the same volume of troposphere.

The other critical modeling assumption is that the propagation loss associated with any zone in a zone group is statistically independent of the propagation loss for any other zone in a different zone group. Therefore, in the model proposed here, the propagation losses associated with any two zones are either perfectly correlated (when both zones are in a common zone group) or statistically independent (when the two zones are in different zone groups). Partial correlation is not included in the model because there exists neither a theoretical model nor an empirical model for partial correlation of propagation losses in the frequency bands of interest.

VI. Aggregate Interference Calculation Using Geometric Partitioning

The problem of calculating the received aggregate interference PSD for a deep-space Earth station from HDFS emitters is drastically simplified when we partition the surrounding area into sectors, zones, and zone groups as shown in Figure 2, where we represent all the emitters in a zone with one equivalent emitter for that zone.

When we compare this partitioned case with the original case shown in Figure 1, we see that the number of emitters has been reduced considerably. Since the locations of the equivalent emitters have been chosen to be the centers of the zones, there is a certain approximation in the realignment of the emitters. These simplifications can be used to rewrite the aggregate interference of Equation (1) as

$$S = \sum_{n=1}^{K} G_n \sum_{m=1}^{M_n} A_{nm} \cdot \frac{1}{L_{nm}(p_n)} \tag{2}$$

where K is the number of zone groups, G_n is the common receiver gain toward the n-th zone group, M_n is the number of zones in the n-th zone group, A_{nm} is the AEIRP spectral density of the zone$[n,m]$ (i.e., zone-m in the n-th zone group) toward the deep-space Earth station receiver (W/Hz), and $L_{nm}(p_n)$ is the p_n-th percentile of the propagation loss of the zone$[n,m]$ due to intervening terrain and atmospheric conditions.

In any given zone group, all zones have the same p_n. This is a consequence of the model assumption of perfect correlation between any two propagation losses (associated with different zones) in a common zone group. The statistics of the aggregate interference expressed by Equation (2) can be obtained using Monte Carlo simulations.

A. Monte Carlo Simulations

The complementary cumulative distribution function (CCDF) of the aggregate interference PSD may be determined through Monte Carlo simulation. A typical CCDF curve is shown in Figure 3.

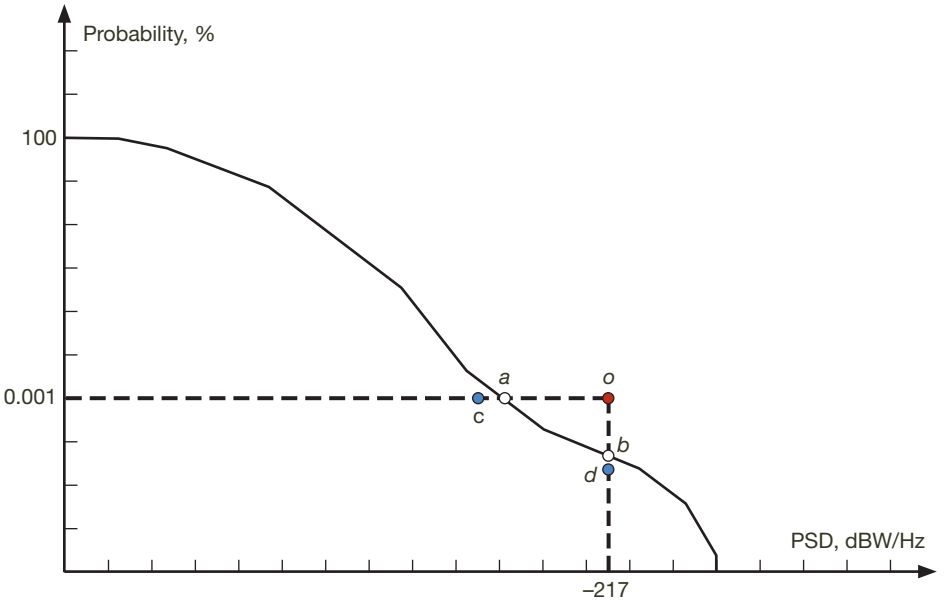

Figure 3. A typical CCDF curve for the aggregate interference received by a deep-space Earth station.

For each iteration of the simulation, a random selection of a set of K propagation loss percentiles p_n, $n = 1, 2 \ldots, K$, is made. Each p_n is a sample of a random variable that is uniformly distributed between 0 and 100, with p_n independent of p_m for $n \neq m$. From these percentiles p_n, the corresponding set of propagation losses is evaluated. For $p_n < 50$, a propagation loss is evaluated using the models in [4]. For $p_n > 50$, the ITU-R models do not characterize propagation loss; in this case, we arbitrarily assumed a symmetric distribution of the propagation loss in units of decibels. Note that since the simulation results are dominated by the small propagation losses corresponding to $p_n < 50$, they are insensitive to the modeling of the large propagation losses corresponding to $p_n > 50$. For the set of propagation losses thus evaluated, a sample value of the aggregate interference PSD is determined by Equation (2). This procedure is iterated millions of times where the sample values of the aggregate interference PSD are collected and counted in order to determine experimentally the CCDF curve for the probability of exceedence.

Also, a numerical technique that employs convolutions may be used to evaluate the statistical distribution of the received interference power spectral density. The results of these simulations or convolutions may be displayed in a CCDF such as in Figure 3.

B. Comparing the Aggregate Interference CCDF with the SRS Protection Criteria

The protection criterion for deep-space Earth stations is shown by point *o* in Figure 3 for the case of 37 GHz, where the protection PSD level is –217 dBW/Hz, not to be exceeded more than 0.001 percent of the time. Note that in the case shown in Figure 3, since the

CCDF curve passes below the protection criterion, the interference is acceptable to the deep-space Earth station, i.e., $Pw(0.001) < -217$ dBW/Hz (point a) or $Pr(-217) < 0.001\%$ (point b). Here, the function $Pr(x)$ is defined as the probability that $S > x$ dBW/Hz and the function $Pw(x)$ is defined as the interference power spectral density with $x\%$ exceedence probability.

As seen from Figure 3, to determine if the interference met the protection criterion, we did not use the whole CCDF curve for the interference power spectral density, but only point a or point b. Therefore, we only need to estimate the values of $Pw(0.001)$ or $Pr(-217)$. In the following section, we describe two methods to estimate these values.

A Monte Carlo determination of the CCDF of the aggregate interference PSD is time consuming, especially so for $p = 0.001$. In order to get an adequate statistical sampling, tens of millions of iterations would be required. Simulations were done in a few example cases. In general, however, it is desirable to have an approximation available that will evaluate quickly on a spreadsheet, in order to foster interactive explorations of potential AEIRP spectral densities and their compatibility with the protection criteria. Two methods of approximation are discussed below.

C. Approximate Aggregate Interference Calculations

This section describes two approximations to estimate the aggregate interference and to determine if the SRS protection criterion is exceeded or not. These are the sum-of-PSDs method, which is used to estimate the value of $Pw(0.001)$, and the sum-of-probabilities method to estimate the value of $Pr(-217)$. Since these are approximate methods, they will usually not give exactly the same values obtained by Monte Carlo simulations or probability-density convolutions. In Figure 3, we have indicated the results of these approximate methods as point c and point d (different from point a and point b). The advantage of these estimates is that they are easily computed and visualized with a spreadsheet.

Sum-of-PSDs Method. To introduce the approximate methods, let us first introduce the following function, $Q_n(p)$, to be the value of the interference PSD contributed by the n-th zone group that is exceeded p percent of the time:

$$Q_n(p) = G_n \sum_{m=1}^{M_n} A_{nm} \cdot \frac{1}{L_{nm}(p)}, \quad n = 1, 2, \cdots, K \tag{3}$$

Note that because of our assumptions about zone groups, the receive antenna gain is fixed since the interference from all the zones of the same zone group enters the receiver antenna at the same off-boresight angle. We also apply the same statistical percentile for all the zones in the zone group, since perfect correlation is assumed between any two propagation losses associated with zones in any given zone group.

Now we can approximate the aggregate interference PSD received from all zone groups by the following equation, which sums the interference PSDs from all the zone groups, where the k-th zone group is assumed to have $p = 0.001$ and the others to have $p = 50$.

$$S_k(0.001) = Q_k(0.001) + \sum_{\substack{n=1 \\ n \neq k}}^{K} Q_n(50), \quad k = 1,2,\cdots,K \tag{4}$$

This procedure is repeated K times, with each zone group in turn having $p = 0.001$ while all other zone groups have $p = 50$. This results in K estimates. In order to estimate the worst interference PSD received by the deep-space Earth station, we pick the maximum of these K values; i.e., $Pw(0.001)$ is estimated as

$$Pw(0.001) = \max_{k=1,2,\cdots K} \{S_k(0.001)\} \tag{5}$$

This method is called the sum-of-PSDs method. In almost all cases studied at the three DSN sites, this method produced a lower bound of the interference PSD at 0.001 percent.

Sum-of-Probabilities Method. In the sum-of-probabilities method, the probability for the deep-space Earth station to receive an interference PSD from each zone group that exceeds the protection criterion of –217 dBW/Hz is first calculated. Then such probabilities from all the zone groups are summed together to form an estimate of the probability that the received aggregate interference exceeds the same criterion:

$$Pr(-217) = \sum_{n=1}^{K} F_n(-217) \tag{6}$$

where $F_n(x)$ is the CCDF of the interference power spectral density received from the n-th zone group. This approach provides a good approximation when the exceedence probability for each zone group is small (on the order of 10^{-5}). Larger probabilities would cause larger errors. Intuitively, at very low probabilities the individual violations are not likely to happen at the same time, so the probability of at least one violation among K zone groups is approximated by the sum of K probabilities of individual violations. The error of this approximation can be checked by performing a Monte Carlo simulation. In the case of troposcattering, the error can also be checked with numerical evaluation of convolutions. In the Appendix, we evaluate this error in the case of troposcattering.

The CCDF, $F_n(x)$, is related to the $Q_n(p)$ that is defined in Equation (3). As a first step in understanding this relationship, another function related to $Q_n(p)$ should be considered; this new function serves the same role as $Q_n(p)$, but its argument is a probability, rather than a percentage, and its value has units of dBW/Hz, rather than W/Hz. $F_n(x)$ is the inverse of this new function. For the case of troposcattering, $F_n(x)$ is available in analytical form, which makes the implementation of the sum-of-probabilities method relatively easy. In the case of diffraction, $F_n(x)$ is not available in analytical form; rather, the inverse of the $Q_n(p)$ -equivalent function must be found numerically, which greatly complicates the implementation of the sum-of-probabilities method.

Accuracy of the Approximate Methods. Among the numerical methods used in this study, only Monte Carlo simulation (and convolution) can produce probability density distributions of the aggregate interference PSD received at the deep-space Earth station receiver that

are highly accurate for the given model assumptions. We have used the results of Monte Carlo simulation as a reference for judging the accuracy of the sum-of-PSDs method and the sum-of-probabilities method.

Mathematical convolution is also able to produce a true probability density distribution. In practice, however, only interferences propagated by troposcattering have distribution functions amenable to numerical convolution without losing precision. For several example scenarios involving only troposcattering, numerical results were obtained with convolutions, and these results agreed very well with those of Monte Carlo simulations.

The sum-of-probabilities method is a good approximation for the probability of exceeding the protection criterion in the case of interference propagated via troposcattering. The sum-of-PSDs is a good approximation for the PSD at 0.001 percentile of PSD distribution. We can see the comparison with Monte Carlo simulation results given in Figures 7, 9 and 11 in Section X.

VII. Reference Profile for Deep-Space Earth Station

Almost all deep-space tracking trajectories have declination angles ranging from –30 deg to +30 deg. When the aggregate interference received by the deep-space Earth station was evaluated at every point of the tracking trajectory, it was immediately apparent that the aggregate interference increases with decreasing elevation angle, especially at a higher rate of change near the beginning and near the end of the tracking pass. This compelled us to define an antenna pointing reference profile for the deep-space Earth station that would include the terrain elevations, the minimum tracking elevations along the target trajectories, and the low elevation angles in the regions where the targets will rise and set. An example reference profile is shown in Figure 4 for the Robledo deep-space Earth station. Similar reference profiles are defined for the Goldstone and Tidbinbilla deep-space Earth stations. Figure 4 also includes a sample spacecraft trajectory that shows example spacecraft rise and set locations. The rise and set locations for all possible spacecraft trajectories will be included in the reference profile.

For the reference profile, the 7-deg elevation angle is chosen as the lowest elevation angle since the aggregate interference is more severe at 7 deg than at higher elevation angles, and critical deep-space tracking events do happen at 7-deg elevation angle. Comparatively, a critical tracking event is unlikely to happen at 6-deg elevation angle where deep-space tracking sessions normally start and end. Where the local horizon is high and the antenna elevation angle comes within 2 deg of the local horizon, the reference profile is set to follow an elevation angle at 2 deg above the local horizon. The 2-deg separation angle is chosen because the system temperature would start to increase when the separation angle gets smaller.

The reference profile also includes the minimum elevation trajectory for spacecraft that have a tracking pass of at least 6 hr, since anything less would probably be considered not suitable to track (Figure 4).

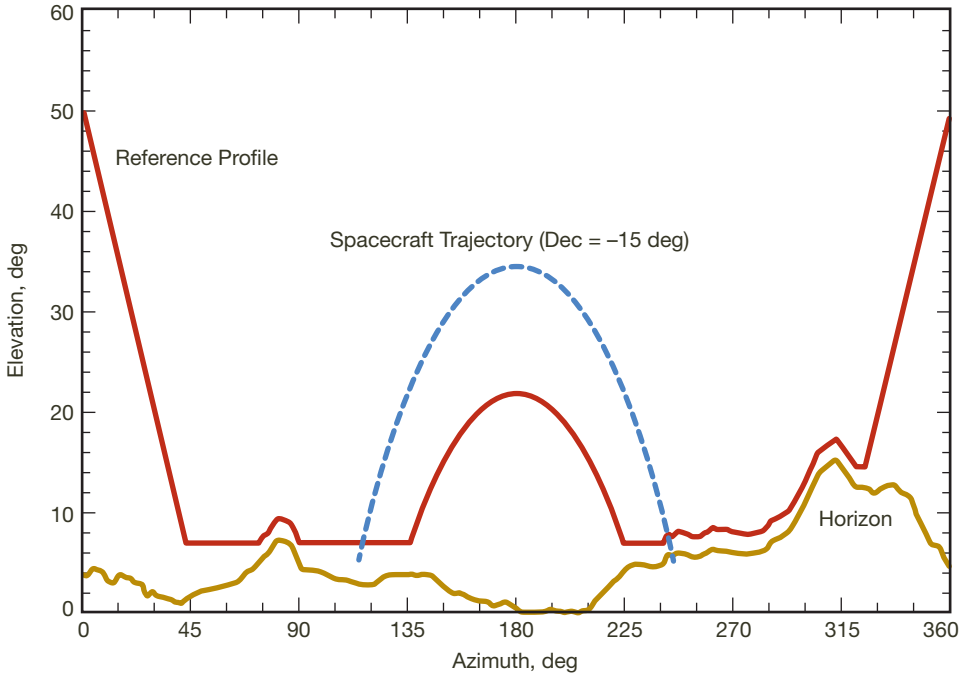

Figure 4. An example reference profile used for the Robledo deep-space Earth station.

We also defined lower and higher reference profiles that are obtained by lowering the reference profile by 1 deg and by raising the reference profile by 1 deg. Later in the article, the estimated aggregate interferences using scans along these reference profiles will be shown in addition to the scan along the nominal reference profile. These scans indicate the sensitivity of the aggregate interference with respect to elevation angle for all the azimuthal directions around the deep-space Earth station. In the text we will refer to these as the lower scan, the higher scan, and the reference scan.

VIII. Interference Potential of Emitters in a Zone Group

If the AEIRP values assigned to individual zones in a zone group are the same, then the aggregate interference given by Equation (2) can be written as

$$S = \sum_{n=1}^{K} A_n \cdot \left[G_n \sum_{m=1}^{M_n} \frac{1}{L_{nm}(p_n)} \right] = \sum_{n=1}^{K} A_n \cdot U_n(p_n) \tag{7}$$

where A_n is the common AEIRP value for the n-th zone group, and U_n is the factor between the brackets, which is called the G/L-factor at p_n % atmosphere for the n-th zone group. Note that the G/L-factor is a function of the pointing direction of the deep-space Earth station antenna, since the gain (G_n) depends on the off-boresight angle. Now, we can easily calculate the interference contribution of the emitters located in the n-th zone group by multiplying the AEIRP of the zone group by its G/L-factor.

We define the *interference potential* of a zone group to be its G/L-factor when the deep-space Earth station antenna is pointed toward the zone group along the reference profile, i.e. the antenna pointing azimuth equals the azimuth angle of the zone group and the antenna pointing elevation equals the elevation angle of the reference profile corresponding to the azimuth of the zone group. Later in this paper we will calculate the interference potentials of all the zone groups at 0.001 percent atmosphere, and will use them to compare and group the zone groups as having lower or higher interference potential. We will refer to the zones in these zone groups as lower potential zones or higher potential zones.

IX. Application of Estimation Methods to DSN Sites

The aggregate interference estimation methods described in Section VI were applied to the NASA DSN sites at Goldstone–USA, Robledo–Spain, and Tidbinbilla–Australia. In each case, the following steps were taken.

The areas surrounding the DSN sites were partitioned into sectors, zones, and zone groups. To illustrate the aggregate interference methods simply, the analysis included densely populated areas surrounding the deep-space Earth stations. It did not include sparsely populated areas. The analysis could be expanded to include more areas if detailed results are desired. For each zone, troposcatter and diffraction losses were calculated at 0.001 percent and 50 percent atmosphere.

After partitioning the surrounding area, the interference potentials for all the zone groups were estimated at 0.001 percent atmosphere. Using these results, we assigned higher AEIRP spectral densities to zone groups with lower interference potential, and lower AEIRP spectral densities to those with higher interference potential. We then finished the distribution of AEIRP spectral densities by assigning AEIRP spectral densities to the zones in the zone groups. This distribution of AEIRP spectral densities to the zones represents a potential HDFS deployment scenario.

The validity of the HDFS deployment scenario was checked by scanning the deep-space Earth station antenna along the reference profile and by comparing the aggregate interference results with the SRS protection criterion. To obtain the maximum AEIRP spectral density assignments while satisfying the SRS protection criterion, the process described above was repeated by adjusting the AEIRP spectral densities.

In addition, we have evaluated the aggregate interference along the lower and the higher reference profiles. These additional scans serve to indicate the sensitivity of the received aggregate interference to the change in elevation angle, as they reveal clearly the effect of terrain on the magnitude of aggregate interference.

X. Results

The analysis results for the DSN sites at Goldstone–USA, Robledo–Spain, and Tidbinbilla–Australia are presented below for the 37-GHz band. The parameters and scenarios assumed

are typical. Actual operational parameters and conditions may differ. Thus, the results should be considered as examples of how to apply the aggregate interference method described in previous sections.

A. Goldstone–USA

The propagation losses from every location within 300 km of the Goldstone deep-space Earth station are given in [7].

Since Goldstone is in the northern hemisphere and most deep-space targets are near the ecliptic plane, the targets are usually in the southern sky of Goldstone. The populated areas in these directions include the southern Mojave Desert and the Los Angeles basin, which lie to the south and to the west of Goldstone. The propagation study indicates that the propagation losses associated with emitter locations in the Los Angeles basin are much larger than the losses associated with Mojave Desert, because of tall mountain ranges between the Los Angeles basin and the Mojave Desert. Therefore, we have separated the area surrounding Goldstone into two different zone groups as the Los Angeles basin and the Mojave Desert.

When a deep-space Earth station in Goldstone tracks a target, these targets come down to 7-deg elevation angle only within the azimuth angle range from 225 deg to 302 deg. The analysis area therefore includes sectors with azimuth angles from 180 deg to 280 deg and radial distances from approximately 50 km to 300 km. No zones are assigned to the mountainous region.

Aggregate interference was then estimated along the reference scan for the Goldstone antenna. The interference potentials of all the zone groups are given in Figure 5 using the troposcatter losses and in Figure 6 using the diffraction losses. These figures show that the interference potentials of the zone groups in the Mojave Desert are higher than those in Los Angeles by about 30 dB. Also, they show that the interference potentials are higher for troposcatter losses than for diffraction losses by about 20 dB.

Based on the interference potentials with the dominant troposcattering mode, we have separated the zone groups of the Mojave Desert into two sets: one with higher interference potential, and the other with lower interference potential. Similarly we have separated the zone groups of Los Angeles into two sets as shown in Table 1. Table 1 also shows the assigned AEIRP spectral densities, which are the highest possible for the four defined sets of zone groups that satisfy the SRS protection criterion along the reference scan.

The sum-of-probabilities method was used to estimate the probability that the received aggregate interference using troposcatter losses exceeded the SRS protection criterion. The results appear in Figure 7. For 230-deg and 250-deg azimuth angles along the reference scan, the probability of exceedence was also evaluated by Monte Carlo simulation. As shown in Figure 7, these two points agree very well with the estimates from the sum-of-probabilities method.

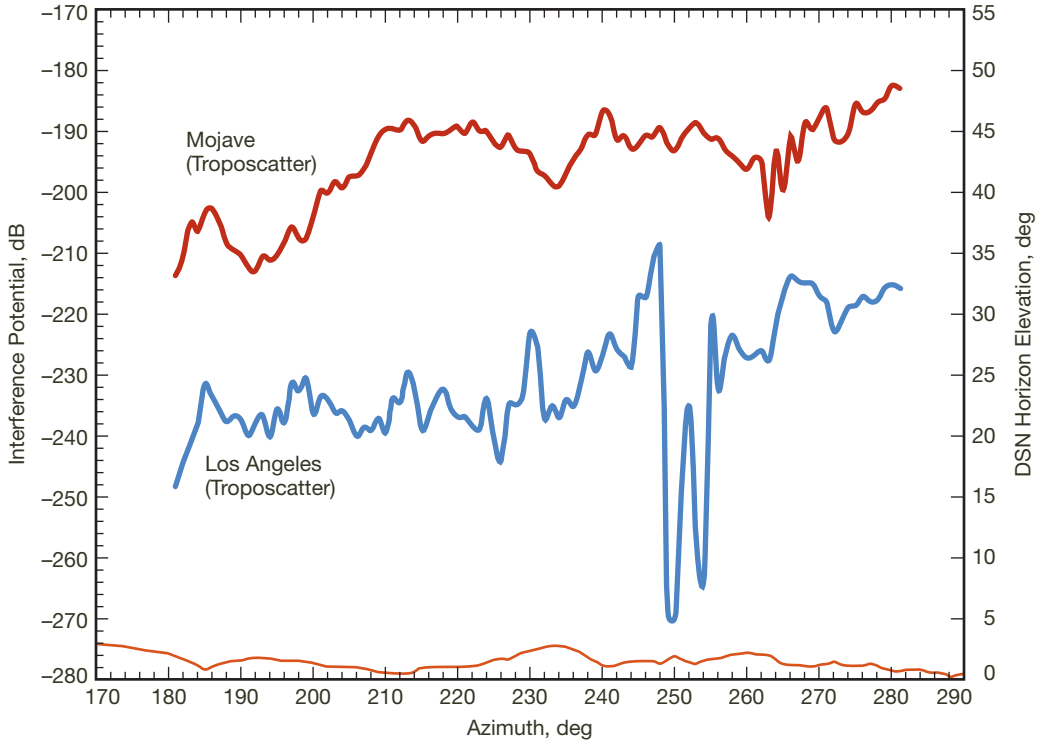

Figure 5. Interference potential of individual zone groups in the Mojave Desert and Los Angeles using troposcatter losses at 0.001 percent atmosphere.

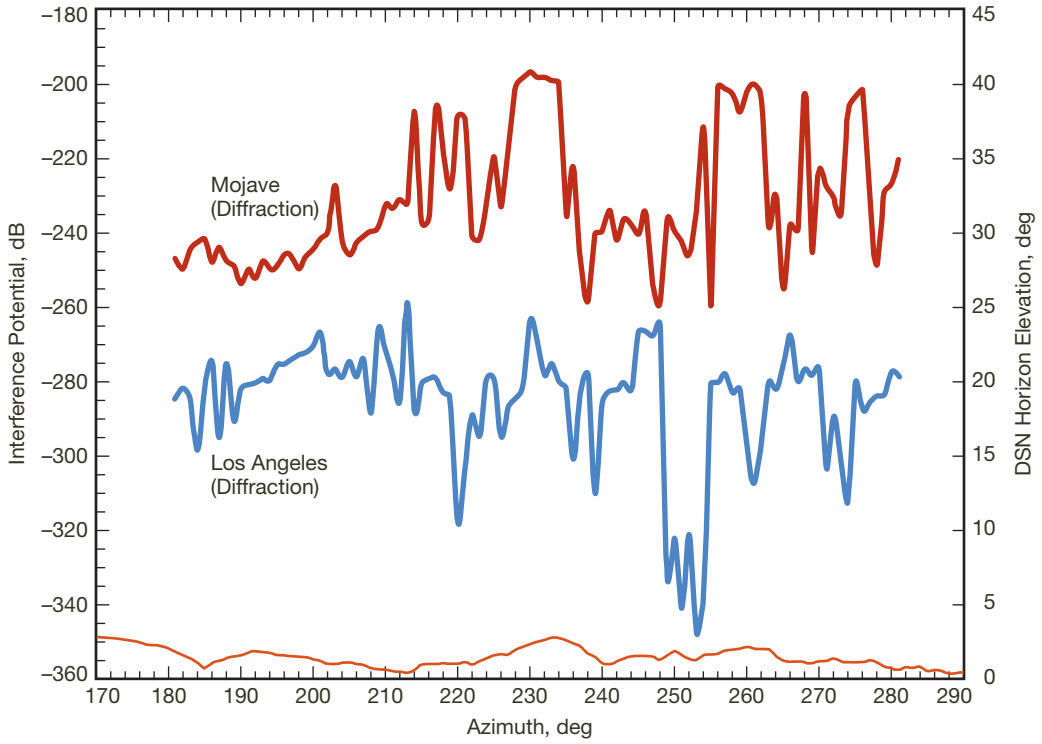

Figure 6. Interference potential of individual zone groups in the Mojave Desert and Los Angeles using diffraction losses at 0.001 percent atmosphere.

Table 1. AEIRP spectral density limits to prevent interference at 37 GHz exceeding protection criteria at Goldstone.

Goldstone	Set of Sectors (Using Sector Identifiers)	AEIRP Spectral Density Limit, dbW/Hz/Zone
Mojave higher potential zones	202–222, 274–280	–39
Mojave lower potential zones	180–201, 223–273	–33
Los Angeles higher potential zones	244–248, 263–280	–10
Los Angeles lower potential zones	180–243, 249–262	3

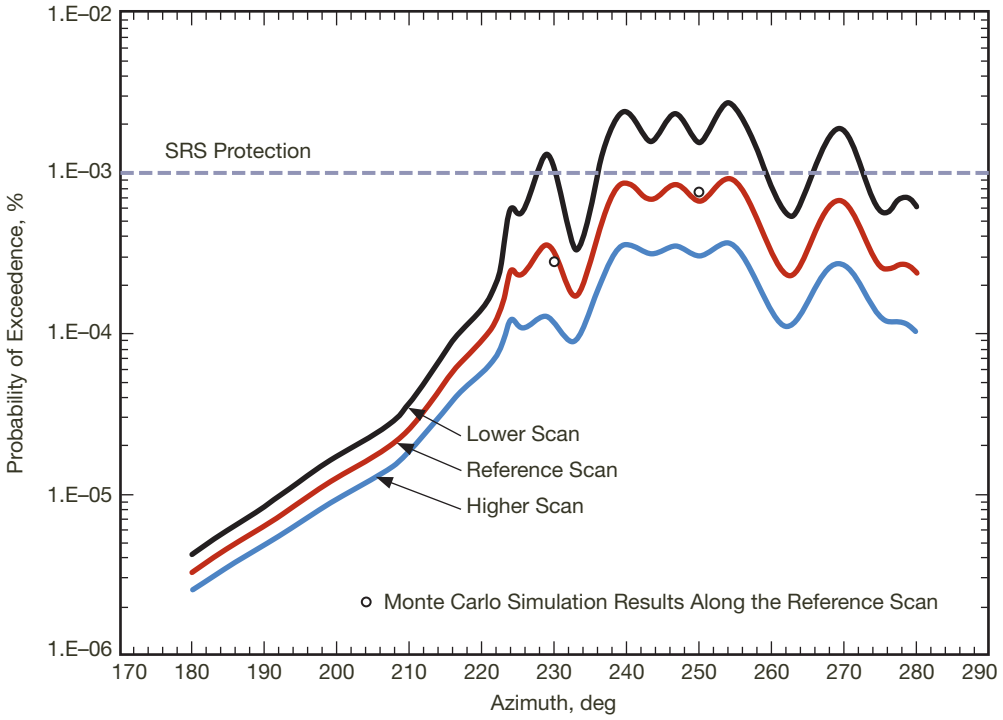

Figure 7. Probability of exceedence for aggregate interference using troposcatter losses at Goldstone (AEIRP densities as defined in Table 1).

If needed, more sets of zone groups could be defined in order to obtain somewhat higher AEIRP spectral density limits. The advantage, however, diminishes with an increasing number of sets.

B. Robledo–Spain

Propagation losses from every location within 300 km of the Robledo deep-space Earth station are given in [7]. Given the large propagation losses in the west, north, and in farther areas in the east due to terrain, we have chosen to focus the analysis to the east of Robledo. The area south of the deep-space Earth station is not included because of its low population density. The analysis area for this study therefore encompasses azimuth angles from 70 deg to 115 deg and radial distances from 30 km to 62 km, including mainly the Madrid region. The analysis area can be easily expanded to include more azimuth angles.

Interference potentials using the diffraction losses and the troposcatter losses were calculated and compared in Figure 8. It is evident that the interference potentials for the diffraction losses are higher than for the troposcatter losses by 10 dB or more for most of the zone groups studied, including those with the highest interference potentials.

Based on the interference potentials using the diffraction losses, we have divided the zone groups in the analysis area into two sets: one with higher interference potential, and the other with lower interference potential as shown in Table 2.

The aggregate interference using diffraction losses is presented in Figure 9, obtained by using the sum-of-PSDs method. Two highest-possible AEIRP spectral densities were chosen for all the zones: –41.3 dBW/Hz for the zones with higher interference potential and –38.3 dBW/Hz for the zones with lower interference potential (Table 2).

The aggregate interference PSD was also calculated for 79-, 90-, 95-, 100-, and 110-deg azimuths along the reference scan by means of Monte Carlo simulation. These data points are shown in Figure 9. In comparing the results obtained by simulation and by the sum-of-PSDs method, we find that the sum-of-PSDs method provides very close estimates of the aggregate interference due to diffraction.

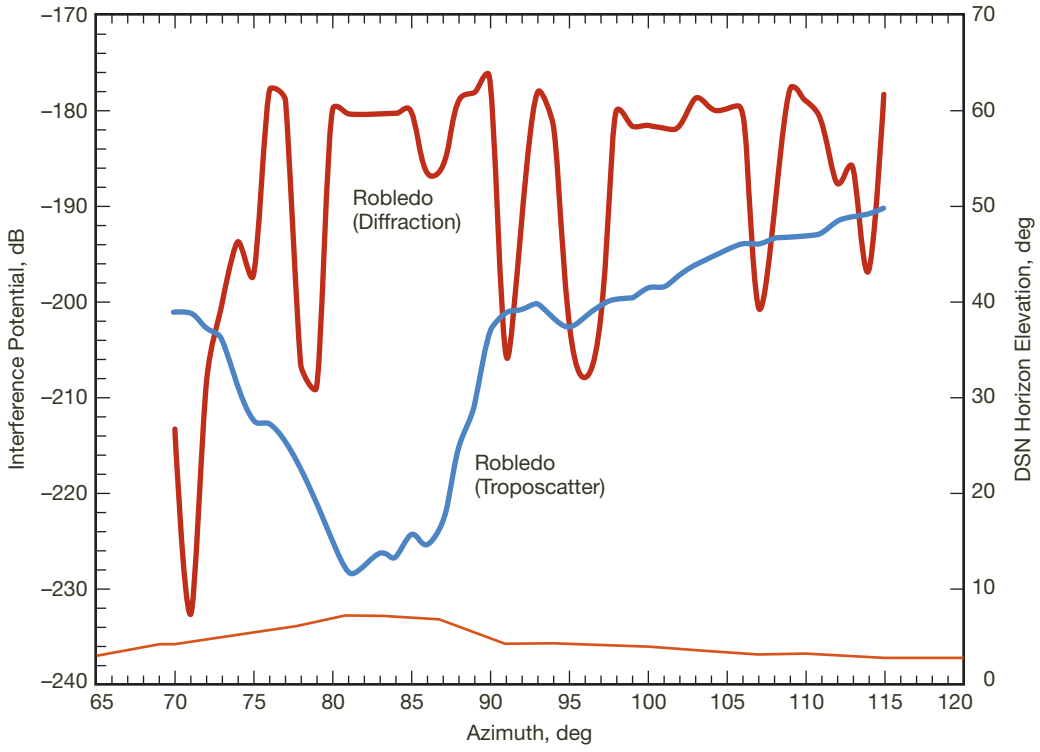

Figure 8. Interference potential of individual zone groups at Robledo using diffraction and troposcatter losses at 0.001 percent atmosphere.

Table 2. AEIRP spectral density limits to prevent interference at 37 GHz exceeding protection criteria at Robledo.

Robledo	Set of Sectors (Using Sector Identifiers)	AEIRP Spectral Density Limit, dbW/Hz/Zone
Lower potential zones	70–75, 79–87, 94–102, 106–108, 111–113	–38.3
Higher potential zones	76–78, 88–93, 103–105, 109–110, 114–115	–41.3

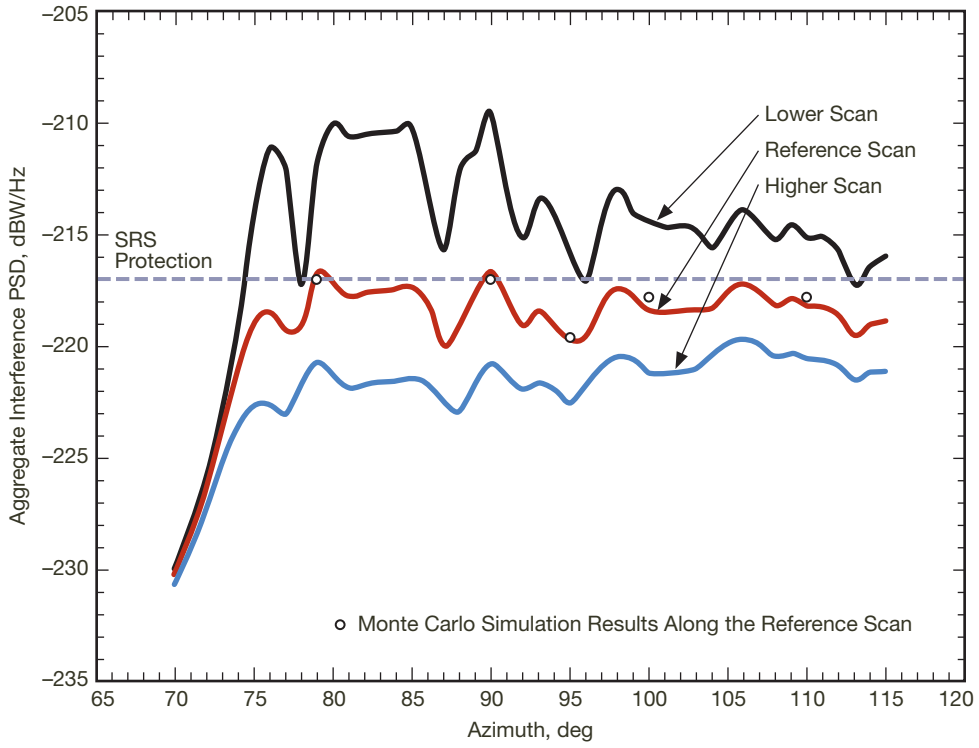

Figure 9. Aggregate interference PSD received at Robledo using diffraction losses (AEIRP densities as defined in Table 2).

Note that if we further subdivide the zone groups into more than two sets, we can get a somewhat higher AEIRP spectral density limit for some zone groups. However, the benefit diminishes as the number of defined sets increases.

C. Tidbinbilla–Australia

Propagation losses from every location within 300 km of the Tidbinbilla deep-space Earth station are given in [7]. We have chosen areas to the north and to the east as the analysis area, including the city of Canberra, because they are densely populated and have major commercial activities. The analysis area encompasses azimuth angles from 0 deg to 130 deg and radial distance from 8 km to 28 km, including five zones per zone group, one zone group per sector.

Figure 10 presents the interference potentials using the diffraction losses and the troposcatter losses. The figure shows that interference potential using diffraction losses are higher than the interference potential using the troposcatter losses by about 17 dB for most zone groups. Based on interference potentials for diffraction case, two sets of zone groups are identified: one having a higher interference potential, and the other having a lower interference potential, as shown in Table 3.

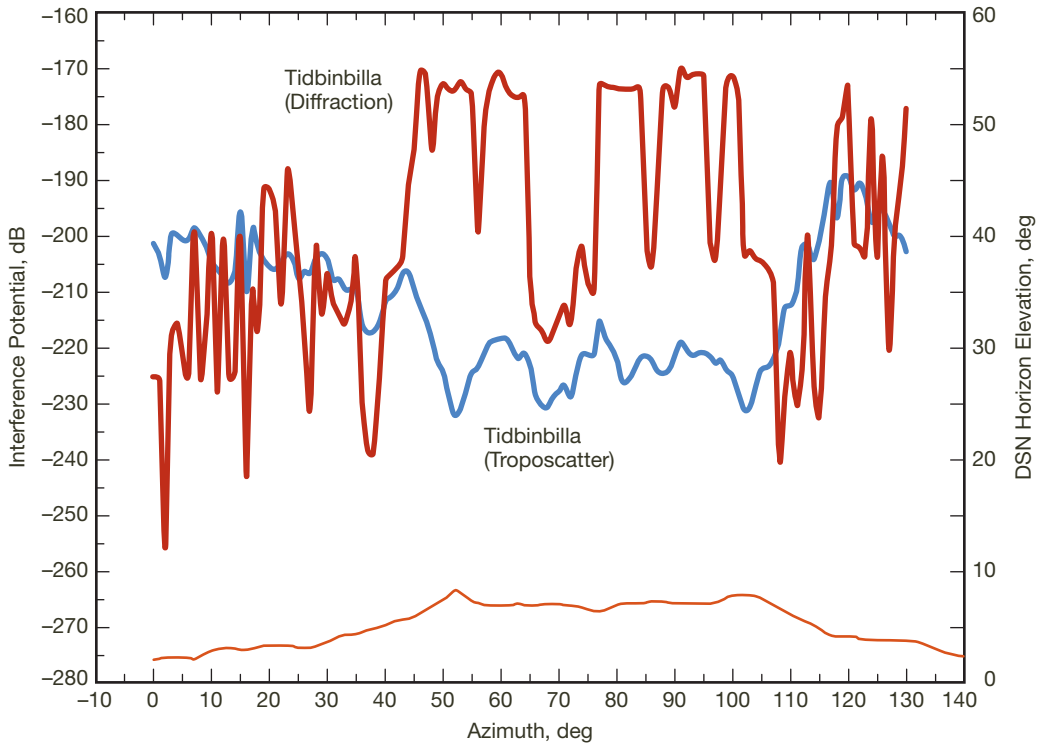

Figure 10. Interference potential of individual zone groups at Tidbinbilla using diffraction and troposcatter losses at 0.001 percent atmosphere.

Table 3. AEIRP spectral density limits to prevent interference at 37 GHz exceeding protection criteria at Tidbinbilla.

Tidbinbilla	Set of Sectors (Using Sector Identifiers)	AEIRP Spectral Density Limit, dbW/Hz/Zone
Lower potential zones	0–17, 26–54, 66–76, 103–117	–35
Higher potential zones	18–25, 44–65, 77–102, 118–130	–47.5

Figure 11 presents the aggregate interference PSD for diffraction received by the deep-space Earth station by scanning along the reference profile. These results are obtained by assigning –47.5 dBW/Hz AEIRP spectral density value to the zone groups with higher interference potential, and –35 dBW/Hz AEIRP spectral density value to the zone groups with lower interference potential. These values were obtained by estimating the aggregate interferences using reference scans, and maximizing them while satisfying the SRS protection criterion.

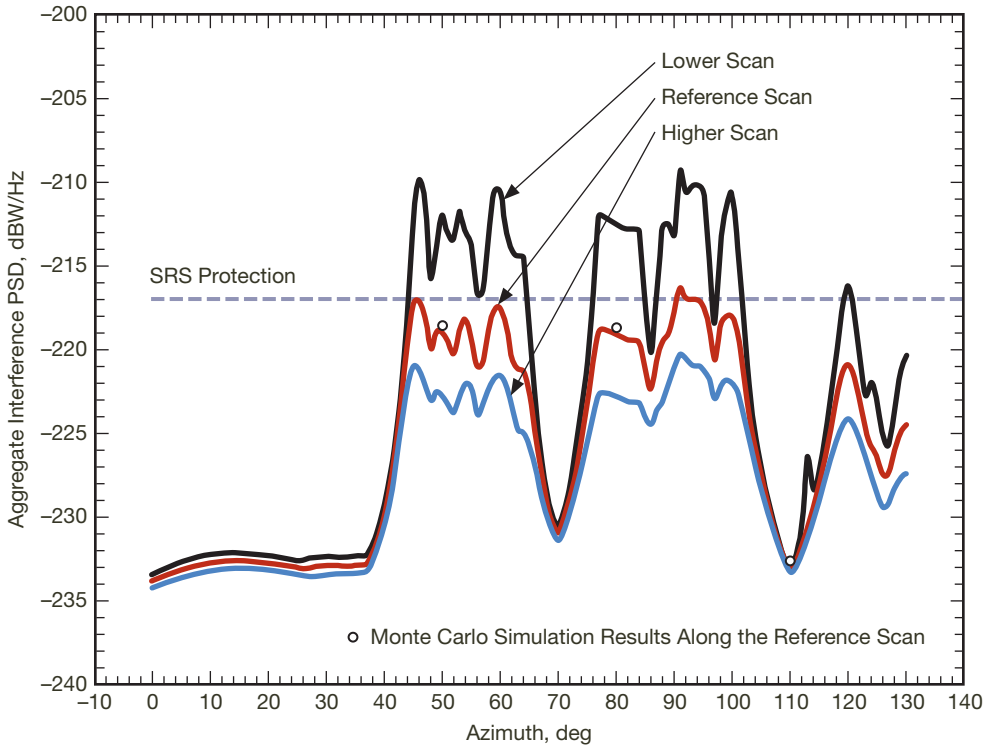

Figure 11. Aggregate interference PSD received at Tidbinbilla using diffraction losses (AEIRP densities as defined in Table 3).

The aggregate interference PSD was also calculated for 50-, 80-, and 110-deg azimuths along the reference scan by means of Monte Carlo simulation. The approximations obtained from the sum-of-PSDs method agree reasonably well with the results of the simulation.

In conclusion, the AEIRP spectral density limits in various azimuth angle ranges needed to protect the deep-space Earth station at Tidbinbilla are given in Table 3.

XI. Number of Emitters

For the purpose of planning HDFS deployment, it is important to estimate the number of emitters per zone (or the number of emitters per square kilometer). There are two separate considerations that lead to limits on the number of emitters. First, the interference to a deep-space Earth station must be kept below the protection level. Second, the self-interference of the HDFS deployment must be kept manageable. (Self-interference in a deployment occurs when fixed service terminals experience interference from other fixed service terminals.)

A. Interference to the Deep-Space Earth Stations

Each emitter in a zone has an EIRP spectral density in the direction of propagation toward the deep-space Earth station, and the AEIRP spectral density for that zone is the sum of these EIRP spectral densities. This AEIRP spectral density is readily calculated if the individ-

ual EIRP spectral densities are known. Prior to deployment, however, these quantities are not known and it becomes advantageous to consider limits to the AEIRP spectral density.

Section X gives examples of limits on the AEIRP spectral density. These limits are based on the protection criteria of the deep-space Earth station. By making assumptions about the transmit PSD and the antenna gain of the emitters, it is possible to translate these limits on the AEIRP spectral density to limits on the number of emitters per zone. The emitter antenna gain pattern should be modeled in accord with [9].

Two methods are described here for estimating the limit to the number of emitters per zone. In the first method, all emitter antennas are assumed to point toward the deep-space Earth station, a worst-case assumption. In the second method, the emitter antennas are assumed to point randomly (within the horizontal plane).

If we assume that all the antennas are pointed toward the deep-space Earth station, and also assume that each emitter EIRP spectral density is 28 dBW/Hz (the maximum allowed in the ITU Radio Regulation for coordination between the fixed service and space research service [10]), the estimated limits would be 65 emitters per zone in the Los Angeles basin, 0.08 emitters per zone in the Mojave Desert, 0.05 emitters per zone in Robledo, and 0.01 emitters per zone in Tidbinbilla. Here, the specified AEIRP spectral densities are –10 dBW/Hz for Los Angeles, –39 dBW/Hz for the Mojave Desert, –41.3 dBW/Hz for Robledo, and –47.5 dBW/Hz for Tidbinbilla, as obtained earlier in the article. Note that these limits on the number of emitters per zone are given only for the high-interference-potential zones. The low-interference-potential zones can, of course, have a higher number of emitters per zone.

If, on the other hand, we assume that the antennas are pointed randomly and we use the model of [3], the estimated limits would be 9000 emitters per zone in the Los Angeles basin, 17 emitters per zone in the Mojave Desert, 14 emitters per zone in Robledo, and 8 emitters per zone in Tidbinbilla. Here, the specified AEIRP spectral densities are the same as in the previous paragraph.

Note that although random pointing leads to an interesting upper bound, it is not a valid assumption for planning real deployment. After the emitters are installed in a zone, the actual AEIRP no longer depends on pointing angles as a random variable, but pointing angles as deterministic. Furthermore, the value of AEIRP increases drastically if one antenna points very close to the direction of propagation toward the deep-space Earth station.

With the geometric partition employed in this article, the zone size increases proportionately with the distance of the zone (center) from the deep-space Earth station. A more useful limit might therefore be the number of emitters per square kilometer. A translation from the number of emitters per zone to the number of emitters per square kilometer may easily be performed by accounting for the size of the zones.

The two sets of estimates discussed here (based on worst-case pointing and random pointing of the emitter antennas) provide us with practical guidance in determining the limits

on the number of emitters per zone. It must be borne in mind that our analysis does not include the effects of multipath or uncertainties in the propagation model, in the terrain, or in the pointing directions. Due to these factors, there is a variance in the actual interference PSD. This variance is not known, but it must be considered in the protection of the deep-space Earth station. Thus, we might need to lower the specified AEIRP spectral density limits by a certain amount to include these uncertainties, or specify a cone angle of avoidance by which the pointing direction of each emitter antenna should keep away from the deep-space Earth station. To quantify these expected uncertainties, we need to do some on-site measurements.

B. HDFS Self-Interference

As the number of emitters increases, the mutual interference between the HDFS emitters becomes important. A study carried out for the European Electronic Communications Committee has indicated that self-interference is a problem when there is (approximately) more than one emitter per square kilometer. This conclusion is based on system parameters applicable to Europe [11]. The results of this study need to be compared with the limits on the number of emitters to protect the deep-space Earth station to see if these new limits represent an additional restriction to the HDFS network. Further work from the fixed service community is needed to confirm the conclusions of [11].

XII. Conclusions

A method of estimating the aggregate interference from the HDFS emitters to a deep-space Earth station is introduced that uses two approximations called sum-of-PSDs and sum-of-probabilities. Given any deployment scenario of HDFS emitters, represented by a geographical distribution of the AEIRP spectral densities, this method estimates if the received aggregate interference would exceed the protection criteria of the deep-space Earth station. In case the deployment scenario would cause excessive interference to spacecraft tracking, this method can be used to find necessary reductions of the AEIRP spectral densities to ensure compatibility.

This method can also be used to find the interference potentials of different zone groups. An HDFS planner can use these interference potentials in assigning suitable AEIRP spectral density limits to different zone groups. These AEIRP spectral density limits would ensure that the aggregate interference received by the deep-space Earth station does not exceed the protection criteria when the deep-space Earth antenna is pointed at any point along the reference profile.

This method was used to calculate the AEIRP spectral density limits for the surrounding areas of the DSN sites at Goldstone, California; Robledo, Spain; and Tidbinbilla, Australia. For Robledo and Tidbinbilla, diffraction is found to be the dominant mechanism of interference propagation, and for Goldstone, tropospheric scattering is found to be dominant mechanism. Further, to estimate the aggregate interference with better accuracy, the sum-of-PSDs approximation should be used in diffraction loss cases and the sum-of-probabilities approximation should be used for troposcatter loss cases.

Once AEIRP spectral density limits are determined, limits on the number of emitters per zone can be found by making assumptions about the transmit power and antenna pointing of the emitters. These limits can then be used to guide the planning of HDFS deployment to ensure compatibility with the SRS.

There will also be limits on the number of emitters per square kilometer that arise from considerations of self-interference in the fixed service. More work is needed to allow conclusive comparisons between the limits due to HDFS self interference and those due to SRS protection criteria.

References

[1] International Telecommunication Union, "Protection Criteria for Deep-Space Research," Recommendation ITU-R SA.1157, 1995.

[2] International Telecommunication Union, "Protection Criteria for the Space Research Service in the 37–38 GHz and 40–40.5 GHz bands," Recommendation ITU-R SA.1396, 1999.

[3] International Telecommunication Union, "Methodology for Determining the Aggregate Equivalent Isotropically Radiated Power from Point-to-Point High-Density Applications in the Fixed Service Operating in Bands Above 30 GHz," Recommendation ITU-R F.1765, 2006.

[4] International Telecommunication Union, "Prediction Procedure for the Evaluation of Microwave Interference Between Stations on the Surface of the Earth at Frequencies Above About 0.7 GHz," Recommendation ITU-R P.452-11, 2003.

[5] International Telecommunication Union, "Propagation by Diffraction," Recommendation ITU-R P.526-6, 1999.

[6] International Telecommunication Union, "Methodology to Determine the Probability of a Radio Astronomy Observatory Receiving Interference Based on Calculated Exclusion Zones to Protect Against Interference from Point-to-Multipoint High-Density Applications in the Fixed Service Operating in Bands Around 43 GHz," Recommendation ITU-R F.1766, 2006.

[7] C. Ho, K. Angkasa, P. Kinman, and T. Peng, "Propagation Loss for Trans-Horizon Interferences in the Regions Surrounding Deep Space Network Complexes," *The Interplanetary Network Progress Report*, vol. 42-162, Jet Propulsion Laboratory, Pasadena, California, pp. 1–20, August 15, 2005.
http://ipnpr.jpl.nasa.gov/progress_report/42-162/162J.pdf

[8] International Telecommunication Union, "Generalized Space Research Earth Station and Radio Astronomy Antenna Radiation Pattern for Use in Interference Calculations, Including Coordination Procedures," Recommendation ITU-R SA.509-2, 1998.

[9] International Telecommunication Union, “Reference Radiation Patterns for Fixed Wireless System Antennas for Use in Coordination Studies and Interference Assessment in the Frequency Range from 100 MHz to About 70 GHz,” Recommendation ITU-R F.699-7, 2006.

[10] International Telecommunication Union, “Parameters Required for the Determination of Coordination Distance for a Receiving Earth Station,” Radio Regulations, Appendix 7, Table 8d, Volume 2, Appendices, 2004.

[11] Electronic Communications Committee, “Methodology to Determine the Density of Fixed Service Links,” ECC Report #20, European Conference of Postal and Telecommunications Administrations (CEPT), October 2002.

Appendix

Propagation Loss due to Troposcattering

The propagation loss due to tropospheric scatter can be modeled as given in [4] by

$$L_{bs}(p) = L_{bs}(50) - 10\log h(p) \quad \text{(dB)} \tag{A-1}$$

$$L_{bs}(50) = 190 + L_f + 20\log d + 0.573\theta - 0.15N_0 + L_c + A_g \quad \text{(dB)} \tag{A-2}$$

$$10\log h(p) = 10.1\left(-\log\left(\frac{p}{50}\right)\right)^{0.7} \quad \text{(dB)} \quad \text{for } p \leq 50 \tag{A-3}$$

where $L_{bs}(p)$ is the basic transmission loss, p is the percentage of time that this loss value is not exceeded, L_f is the frequency dependence of the loss, d is the great-circle path distance in kilometers, θ is the angular distance in millirad, N_0 is the sea-level surface refractivity, L_c is the aperture-to-medium coupling loss, and A_g is the gaseous absorption. An important aspect of this model is that the first term, $L_{bs}(50)$, is independent of p and, therefore, deterministic, which shows the dependence of $L_{bs}(p)$ on distance, frequency, and terrain. $L_{bs}(50)$ represents the 50 percent propagation loss. The second term on the right-hand side of Equation (A-1) is random (since it is a function of p) but is independent of distance, frequency, and terrain. This separation of the random influence from the dependencies on distance, frequency, and terrain leads to great simplification in the mathematics.

The random variable $h(p)$, called the signal-enhancement factor, represents the variability of the propagation loss with meteorological conditions. The larger the signal-enhancement factor, the smaller the propagation loss and the larger the received interference. The troposcattering signal-enhancement factor is defined only for $0 \leq p \leq 50$. A complete statistical characterization requires that $h(p)$ be known for all p, $0 \leq p \leq 100$. However, a little numerical experimentation has revealed that the large signal-enhancement factors, corresponding to small values of p, dominate the calculation of aggregate interference PSD. In other words, very nearly the same results are obtained for any reasonable model of $h(p)$ for $50 \leq p \leq 100$ that might be assumed.

The two terms of $L_{bs}(p)$ offer a convenient way of incorporating into the problem statement correlation (or lack of correlation) of propagation losses. The signal-enhancement factor is the same for all zones within a common zone group; this models the perfect correlation of the propagation losses within the zone group. The signal-enhancement factor for one zone is statistically independent from that for another zone in a different zone group; this models the statistical independence of those zones.

The signal-enhancement factor has a large dynamic range. From Equation (A-3), $h(50)$ is 0 dB, and $h(0.001)$ is 29.8 dB. In other words, for any given zone the troposcatter loss is about 30 dB less than its median value for a few minutes each year. This explains, in part, why the sum-of-probabilities method yields a good approximation for troposcattering, where the effect of each zone group upon the received PSD is considered independently

from that of the other zone groups. Such a simplification can be justified only if the contribution of a zone group is much larger for the $p = 0.001$ condition than for the $p = 50$ condition. The dynamic range of diffraction loss, on the other hand, is much smaller than for troposcatter loss; and it has been found that the sum-of-probabilities method does not usually yield a good approximation when diffraction is the dominant propagation mechanism.

A simple example provides insight into the validity of the sum-of-probabilities approximation. This simple example is an idealization, used for the purpose of illustration, and does not represent any real scenario. First, we shall consider an exact calculation of the aggregate interference PSD due to troposcattering. From Equation (A-1), we see that the reciprocal of the dimensionless troposcattering loss is proportional to $h(p)$. Then, from Equation (2) of Section VI, we see that the aggregate interference PSD is a weighted sum of the $h(p_n), n = 1,2,\ldots,K$; each $h(p_n)$ corresponds to a different zone group. We consider the simple case where all the weighting factors equal 1. Hence, in this simple case, the aggregate interference PSD equals an unweighted sum of the K signal-enhancement factors. A Monte Carlo simulation could be done to find the CCDF of the aggregate interference PSD. However, in this simple case, the probability density function of the aggregate interference PSD equals the convolution of the probability density functions of the (random) signal-enhancement factors. The CCDF of the aggregate interference PSD was calculated by means of convolutions, which were implemented as fast convolutions with the aid of fast Fourier transforms. These results are shown (as solid lines) in Figure A-1 for three different values of K: 32, 128, and 512.

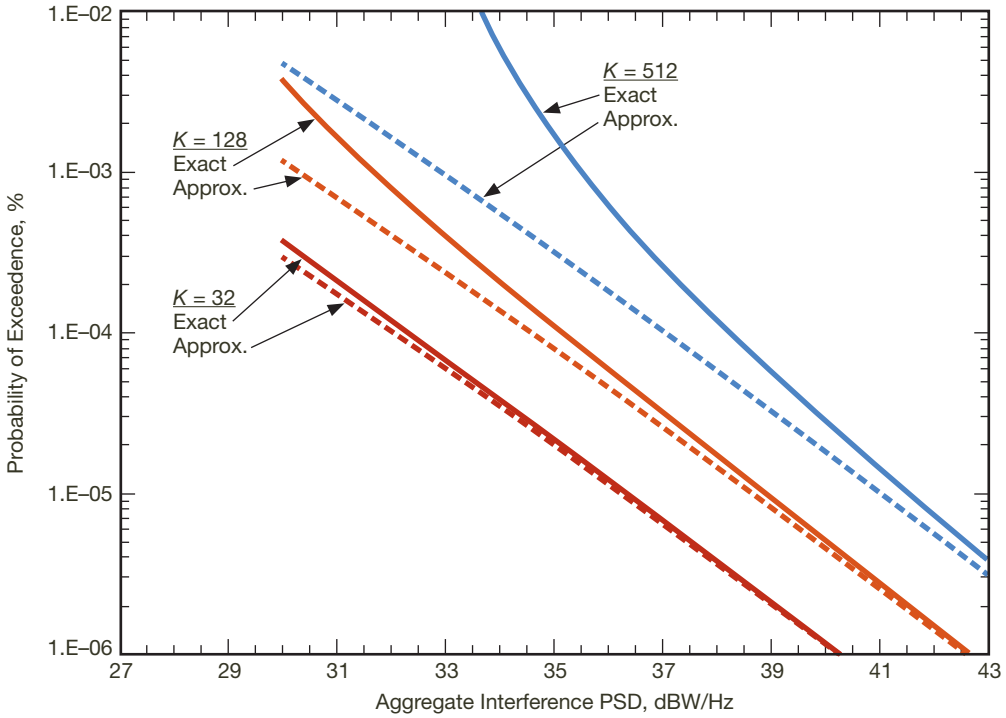

Figure A-1. CCDF of aggregate interference PSD as estimated by the sum-of-probabilities method and as computed (exactly) with convolutions (*K* = number of zone groups).

The sum-of-probabilities method, when applied to this simple example, gives a particularly simple result. The aggregate interference PSD is, in this case, estimated as K times the CCDF of the individual random variable $h(p)$. (Because of the symmetry in this simple example, the sum of K probabilities equals K times the individual probability.) These approximate results are shown (as dashed lines) in Figure A-1 for three values of K: 32, 128, and 512.

Comparing the approximate (sum-of-probabilities) results with the exact results (computed with convolutions), we can make the following observations. For very small probabilities and for K not too large, the sum-of-probabilities method applied to troposcattering yields useful approximations that tend to underestimate the aggregate interference PSD. For a probability of 10^{-3}, the approximation is low by less than 2.5 dB if K is less than 512. For a probability of 10^{-5}, reflecting the actual protection criteria for the SRS, deep space, the approximation is low by less than 0.5 dB if K is less than 512.